



Effect of capping procedure on quantum dot morphology: Implications on optical properties and efficiency of InAs/GaAs quantum dot solar cells



E.C. Weiner^{a,b,*}, R. Jakomin^{b,c}, D.N. Micha^{b,d}, H. Xie^e, P.-Y. Su^e, L.D. Pinto^{a,b}, M.P. Pires^{b,f}, F.A. Ponce^e, P.L. Souza^{a,b}

^a LabSem, CETUC, Pontifícia Universidade Católica do Rio de Janeiro—Rua Marquês de São Vicente 225, Rio de Janeiro 22452-900, RJ, Brazil

^b Instituto Nacional de Ciência e Tecnologia de Nanodispositivos Semicondutores – DISSE – PUC-Rio, RJ, Brazil

^c Campus Duque de Caxias, Universidade Federal do Rio de Janeiro, UFRJ, RJ, Brazil

^d Coordenação de Licenciatura em Física, CEFET/RJ, Petrópolis RJ, Brazil

^e Department of Physics, Arizona State University, Tempe, AZ 85287-1504, USA

^f Instituto de Física, Universidade Federal do Rio de Janeiro, UFRJ, Rio de Janeiro RJ, Brazil

ARTICLE INFO

Keywords:

Quantum dot solar cell
Intermediate band
MOCVD growth
Optoelectronic properties
Photoluminescence
Transmission electron microscopy

ABSTRACT

InAs/GaAs quantum dot solar cell structures have been grown by metal organic vapor phase epitaxy, using partial capping of the quantum dots plus a subsequent thermal anneal. The optical characteristics of the InAs quantum dot layers have been studied as a function of the GaAs capping layer thickness and annealing temperature. We observe that a thinner capping layer and a higher annealing temperature result in lower non-radiative defect density and in improved quantum dot size homogeneity, leading to intense and sharp photoluminescence emission at low temperatures. We use an effective mass approximation model to correlate the photoluminescence emission characteristics to the quantum dot composition and dimensions. The resulting InAs/GaAs intermediate band solar cells show the best performance for the case of a 3 nm thick capping layer and annealing at 700 °C.

1. Introduction

Quantum dot intermediate band solar cells (QD-IBSC) have been proposed in order to overcome the Shockley-Queisser limit in single junction solar cells [1]. This is in principle achieved by forming an isolated intermediate band (IB) that extends the optical absorption to energies within the energy band gap of the matrix [2]. The IB allows additional sub-bandgap absorption from the valence band (VB) to the IB and from the IB to the conduction band (CB). The enhancement of the photocurrent and the preservation of the voltage are expected to result in a 63% efficiency under full sun concentration for optimum energy values of matrix bandgap of 1.95 eV, VB to IB of 1.24 eV and IB to CB of 0.71 eV [3]. The IB may be created by forming discrete energy levels of quantum dots (QDs) embedded in a higher energy gap matrix. High densities of InAs QDs grown on GaAs have been reported for this purpose, resulting from ample previous experience on this material system [4]. However, InAs/GaAs QDs produce an effective experimental bandgap of 1.2 eV and sub-bandgaps of 1.0 eV and 0.2 eV, far from the optimum values [5]. Recently proposed alternative structures of InAs QDs on InGaP [6,7] and on AlGaAs [8,9], with matrix energy gaps of

1.8–1.9 eV, would be better choices in order to approach the ideal combination of energies. However, even without the best theoretical combination of energies, the InAs/GaAs system, most likely because it has been more fully investigated, has demonstrated the highest reported efficiencies among QD solar cells, in some cases overcoming the efficiency of the reference single junction GaAs solar cell [10]. Higher photocurrents and lower open circuit voltage (V_{oc}) have been reported for the InAs/GaAs QD solar cells compared with the single junction GaAs solar cells [11,12]. The lower V_{oc} values have been attributed to the reduction of the effective bandgap due to the presence of quasi-continuum states in the VB and in the wetting layer and to the allowance of thermal escape between the IB and the CB at room temperature.

However, degradation of the cell performance may also be attributed to low optical quality of the QDs, due to the presence of misfit dislocations or other recombination centers in the cell structure [11]. The complexity of this material system is intrinsic to the Stranski-Krastanov growth mode, where a large lattice mismatch between the QDs and the underlying material is necessary. Consequently, the accumulated stress may result in the generation of misfit dislocations by plastic relaxation. Suppression of plastic relaxation during growth is

* Corresponding author at: LabSem, CETUC, Pontifícia Universidade Católica do Rio de Janeiro—Rua Marquês de São Vicente 225, Rio de Janeiro 22452-900, RJ, Brazil.
E-mail address: eleonoracw@cetuc.puc-rio.br (E.C. Weiner).

important in order to improve the optoelectronic properties and the efficiency of the solar cells. A crucial approach resides in the method used to grow the active region, where the presence of 10 or more stacked QD layers interposed with spacer layers of higher energy gap materials is necessary. Thick barrier layers (around 100 nm) may be used to prevent tunnel escape directly from IB to CB [13]. The strategies to avoid plastic relaxation in the thin film structure contemplate strain compensation layers with reduced InAs coverage [10,12] and partial capping methods [14–16]. The former uses layers with opposite lattice mismatch in order to reduce the net strain, while the latter consists in partially covering the QDs with a thin capping layer grown at a low temperature followed by subsequent annealing at a higher temperature. The method, known as *indium flush*, allows the control of the QD height by removing the tip of the QD that protrudes above the capping layer [17,18], thus preventing the formation of QDs with heights above the critical dimension for plastic relaxation [15].

In this work, we study the effect of partial capping parameters (annealing temperature and capping layer thickness) on the QD photoluminescence (PL) peaks. We have fabricated InAs/GaAs QD IBSCs under various capping and annealing conditions. Using a 3D effective mass approximation model, we correlate the PL emission energies to the size, shape and composition of the InAs QDs. We show that a thinner capping layer and a higher annealing temperature produce an IBSC with improved optical quality and photovoltaic performance.

2. Material and methods

The InAs/GaAs IBSC structures were grown by metalorganic chemical vapor deposition in an Aixtron AIX 200 horizontal reactor at 100 mbar on *n*-doped (001) GaAs substrates. Trimethylaluminum (TMAI), trimethylgallium (TMGa), trimethylindium (TMIn) and arsine (AsH₃) were used as aluminum, gallium, indium and arsenic sources. CBr₄ and SiH₄ were used for *p*- and *n*-type doping. The structure of the QD cells, shown schematically in Fig. 1, consists of a *p-i-n* structure with an active region with an adequate thickness to accommodate the QD layers within it and benefit from the low energy photon absorption. In our structure, the entire *i* layer is active, because it is depleted of carriers by the electric field. A reference cell without the QD layers in the active region was designed with the same active region's total thickness.

The growth sequence is the following (see Fig. 1): on the GaAs substrate (2), a 500 nm thick *n*-type ($1 \times 10^{18} \text{ cm}^{-3}$) GaAs buffer layer (3) is followed by a 100 nm thick *n*-type ($3 \times 10^{18} \text{ cm}^{-3}$) Al_{0.3}Ga_{0.7}As back surface field layer (BSF) (4), a 300 nm thick *n*-doped ($2 \times 10^{18} \text{ cm}^{-3}$) GaAs base layer (5) grown at 630 °C and a 90 nm thick undoped GaAs barrier layer (6). Next, is the 1 μm thick active region (7) that consists of ten InAs QD layers, grown at 490 °C, under optimized conditions in order to achieve a high QD density of $1.8 \times 10^{10} \text{ cm}^{-2}$. The active region is described in more detail in the next paragraph. After the

active region, a 100 nm thick *p*-doped ($1 \times 10^{18} \text{ cm}^{-3}$) GaAs emitter layer (8) grown at 570 °C, followed by a 30 nm *p*-In_{0.48}Ga_{0.52}P window layer (9) grown at 630 °C ($1 \times 10^{18} \text{ cm}^{-3}$) and a 30 nm thick *p*⁺-doped GaAs ($4 \times 10^{19} \text{ cm}^{-3}$) contact layer (10). During the processing steps, an anti-reflective coating (11) and *n* (Ti/Ge/Pd/Au) and *p* (Pd/Zn/Au) type ohmic contact layers (1 and 12 respectively) are deposited. In the reference sample, the active region is formed only by a 1 μm thick, undoped GaAs layer, without any QDs.

The QDs are *n*-type, Si doped at $\sim 2 \times 10^{17} \text{ cm}^{-3}$, using conditions calibrated for GaAs films, as we have determined that the Si incorporation in InAs is essentially the same as for GaAs, with only 8% difference. After the QD deposition at 490 °C, an annealing step is performed for 12 s and a GaAs capping layer is grown, both at the same temperature of 490 °C. The GaAs capping thicknesses were 3 nm and 6 nm. The temperature was then raised in order to indium flush those QDs with a height higher than the capping layer thickness. The annealing temperature was 630 °C (for samples labeled 3–630 and 6–630, corresponding to 3 nm and 6 nm thick GaAs capping layers, respectively) and at 700 °C (for samples 3–700 and 6–700, corresponding to 3 nm and 6 nm thick GaAs capping layers). Subsequently, a 90 nm thick GaAs barrier was grown at the same temperature of the indium flush step. The same procedure was repeated for subsequent QD layers. The growth conditions are summarized in Table 1.

Free standing QDs were analyzed using a Veeco MultiMode V AFM in tapping mode. The AFM tip was driven at frequencies higher than 100 kHz. The surfaces were then mapped on $2 \times 2 \mu\text{m}$ topography images, with a height accuracy of 0.5 nm. The morphology of the InAs QDs was studied by scanning transmission electron microscopy (STEM) using a high-angle annular dark-field (HAADF) detector, in an aberration corrected JEOL ARM 200 scanning transmission electron microscope. Both instruments were operated at 200 kV. High resolution X-ray diffraction (HRXRD) were performed using a D8 Discover Da Vinci (Bruker) diffractometer equipped with Cu K_{α1} line and Ge (004) monochromator crystal.

PL spectra were obtained at 15 K, using the 487 nm line of an Ar⁺ laser, a 250 mm monochromator and a germanium nitrogen-cooled photodetector. Photovoltaic devices were processed as 0.0547 cm² mesa structures using conventional photolithography. A full area ohmic metal contact was deposited at the rear side of the cells and a finger structure of ohmic metallic contact covering around 10% of the surface was defined at the front side. Complementary to the area of the fingers, a double layer MgF₂/Ta₂O₅ anti-reflective coating was deposited. Current density-voltage (*J-V*) curves were measured under standard test conditions, namely 25 °C and 1 sun (AM 1.5 G). External quantum efficiency (*EQE*) curves were obtained from spectral response measurements under light bias, at 25 °C and under short circuit conditions. The *EQE* curves were normalized to absolute values using the short circuit current values from the light *J-V* characteristics obtained previously.

3. Results and discussion

3.1. Structural analysis

An AFM image of free standing InAs QDs grown on a GaAs substrate, following the previously described conditions, is shown in Fig. 2(a). The QD main height is between 2 and 3 nm although QDs higher than

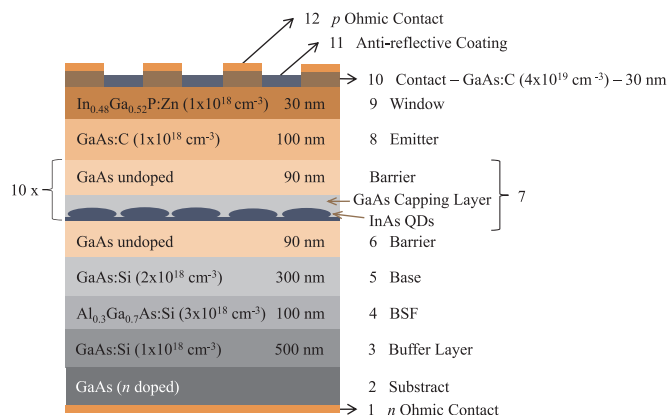


Fig. 1. Schematic diagram of the InAs QD solar structure.

Table 1
Growth conditions for the QD structures investigated in this reported work.

Solar cell	Cap layer thickness (nm)	Indium flush temperature (°C)
3–630	3	630
6–630	6	630
3–700	3	700
6–700	6	700

Download English Version:

<https://daneshyari.com/en/article/6534374>

Download Persian Version:

<https://daneshyari.com/article/6534374>

[Daneshyari.com](https://daneshyari.com)